Energy Mismatch and Cutoff Waves in a Two-Dimensional Space-Charge Flow*

J. E. ROWE AND R. Y. LEE
Department of Electrical Engineering, University of Michigan, Ann Arbor, Michigan
(Received March 10, 1961)

A general treatment of the input boundary value problem for two-dimensional space-charge flow is developed using a theory of electrostatics (Thomson's) which notes that in an electrostatic problem the electric field distribution is such that the electrostatic-field energy is a minimum. This principle is used to determine the average energy density mismatch and the starting conditions for finite thickness beams in M-type backward-wave oscillators. It is shown that the mismatch is greatest for strong space-charge fields, high-circuit attenuation, and signal frequencies below the cyclotron frequency. The starting length and beam velocity are greater as calculated by the variational procedure than obtained by the approximate method. Under certain conditions the average energy density mismatch is greater than 20% of the electrostatic field energy in the absence of the beam.

INTRODUCTION

MANY authors[1–6] have analyzed a system of space-charge flow in a crossed-field environment between planar electrodes. The procedure is to solve the eigenvalue problem defined by the transverse boundary conditions applied to a simultaneous solution of the circuit, Poisson, and Lorentz equations for the system. The eigenvalues of the secular equation are the propagation constants for the waves in the system. The total wave system is made up of three near-synchronous waves and two cyclotron waves. It has been shown that under conditions in which the near-synchronous waves are of interest the cyclotron waves are excited to a negligible extent. This reduces the system to a three-wave system and thus considerably simplifies the treatment of the input boundary value problem.

The subject and main thesis of this paper is a treatment of the energy mismatch at the input boundary and subsequent excitation of cutoff waves in a planar M-type space-charge flow. The treatment is particularly applied to a consideration of the effect of this mismatch on the starting conditions in an M-type backward-wave oscillator (M-BWO). The method is a general one and can be applied to other flow systems, such as E type.

Most of the authors cited have handled the input boundary value problem and the calculation of the excited wave amplitudes by matching the boundary conditions at just one or two levels of the flow at the input boundary. In all two-dimensional space-charge flows in which the velocity may vary across the flow, this is obviously an approximate treatment. Particularly in thick-beam devices (the term "thick beam" is here used to indicate that the beam occupies an appreciable fraction of the interaction width and, hence, there may be an appreciable variation of velocity across the beam in a two-dimensional flow), this energy density mismatch can lead to erroneous calculations of starting current. Hershenov[5] has used a fundamental theorem of electrostatics[7] (Thomson's theorem) to justify the minimization of the energy in the cutoff waves, because in an electrostatic problem the electric field distribution is such that the electrostatic-field energy is a minimum. He applied this treatment to the M-type slipping stream flow in an amplifier, wherein a field analysis was used. The justification for using this theorem of electrostatics in treating cutoff waves is that the wave equation may be replaced by Laplace's equation when the region being considered is small compared to a wavelength and, hence, retardation terms may be neglected.

This study considers the energy mismatch and excitation of cutoff waves in an M-type flow interaction with a backward circuit wave. The method of analysis utilizes the equivalent circuit approach of Dombrowski[4] to obtain the eigenvalues of the system, and then the excited wave amplitudes for the near-synchronous waves are calculated using the minimum-energy method. A comparison of calculated starting current is made using both this method and the simpler treatment of the input boundary value problem. A variational method for minimizing the excitation of cutoff waves is developed quite generally and may readily be applied to other two-dimensional space-charge flow systems, such as that used in single-transit electrostatically focused systems.

NEAR-SYNCHRONOUS WAVE DISPERSION EQUATION

A general solution of the eigenvalue problem defined by the flow system considered and the usual boundary conditions gives rise to a fifth-order dispersion equation. Three of these waves are called the near-synchronous waves and the other two are the cyclotron waves. Dombrowski studied this composite system by applying

* This work was supported by the U. S. Signal Corps under contract.

[1] O. Buneman, Nature **165**, 474 (1950).

[2] G. G. MacFarlane and H. G. Hay, Proc. Phys. Soc. (London) **B63**, 407 (1950).

[3] R. W. Gould, J. Appl. Phys. **28**, 599 (1957).

[4] G. E. Dombrowski, Tech. Rept. No. 22, Electron Physics Laboratory, University of Michigan, Ann Arbor, Michigan (October, 1957).

[5] B. Hershenov, Tech. Rept. No. 29, Electron Physics Laboratory, University of Michigan, Ann Arbor, Michigan (March, 1959).

[6] B. Hershenov, Trans. IRE on Electron Devices **ED-7**, 163 (1960).

[7] J. A. Stratton, *Electromagnetic Theory* (McGraw-Hill Book Company, Inc., New York, 1941), p. 114.

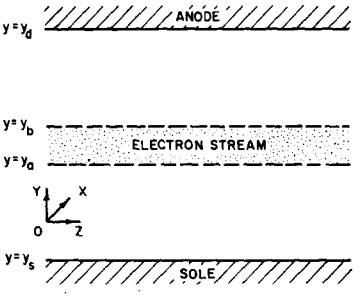

FIG. 1. Configuration and coordinate system used in the analysis.

five boundary conditions at the input and calculated the amplitudes of the five waves excited. As boundary conditions he matched the two velocity components and the y displacement at the center of the stream, and the two electric field intensity components at the anode. As a result he found that both cyclotron waves were excited to a negligible extent and, hence, the third-order near-synchronous dispersion equation could be used with excellent results. Dombrowski's method of derivation was essentially an equivalent circuit method as opposed to Gould's admittance matching technique. Other differences occurred in the treatment of the input boundary value problem and other details of the analysis, but the results for the near-synchronous wave dispersion equation were the same.

The form of the dispersion equation used in studying the excitation of near-synchronous and cutoff waves in the assumed planar magnetron space-charge flow is given below. The equation has been generalized from Dombrowski's to include the effects of circuit loss and the conventional $\delta_n=x_n+jy_n$ has been used for the complex propagation constants of the system.

$$\delta^3-j\left[2r\left(\frac{H-1}{H+1}\right)+(b+jd)\right]\delta^2$$

$$-\left[r^2+2r(b+jd)\left(\frac{H-1}{H+1}\right)-1\right]\delta+j(b+jd)r^2=0, \quad (1)$$

where $H=\tanh j\Gamma(y_d-y_b)/\tanh j\Gamma(y_a-y_s)$, beam position parameter, d=the circuit loss parameter, b=injection velocity parameter, and $r=s_u/D_i$, the space-charge parameter defined as the ratio of the velocity spread in the beam to the interaction parameter. This is a third-order equation and the roots for a given set of H, r, d, and b are the perturbation propagation constants for the near-synchronous waves in the system. This equation is for the M-type backward-wave oscillator and will be used later in the analysis.

The space-charge parameter, S, of Gould is related to the r used here, and in fact for a Brillouin flow ($\omega_p=\omega_c$) they are equal. The minimum-energy method will be used to calculate the amplitudes of the near-synchronous waves excited as well as the cutoff waves, and the energy density associated with the mismatch will be determined.

ENERGY MISMATCH EQUATIONS

It was pointed out above that a more satisfactory procedure for handling the input boundary value problem has been developed by Hershenov[5] in his small-signal field analysis of the magnetron amplifier. If only propagating modes are considered at the input boundary plane, then there will be a mismatch present, which is accounted for by an infinite spectrum of non-propagating or cutoff modes. The cutoff waves are accounted for by minimizing the energy density associated with the mismatch in the presence of the stream. This technique is based on the application of Thomson's[7] theorem, which states that in an electrostatic problem the electric field distribution is such that the electrostatic field energy is a minimum. The presence of the electron stream between the rf structure and the sole electrode perturbs the boundary conditions and a variational procedure is used to calculate the excited wave amplitudes with a minimization of the energy density associated with the cutoff waves. This minimization amounts to minimizing the mean-square mismatch across the stream boundary at $z=0$.

In the study to be made here the variational technique is to be applied, using a circuit type of analysis, to the study of the energy mismatch and the effect of cutoff waves in planar M-type backward-wave oscillators as one special case of a two-dimensional flow system. This procedure is particularly useful when there is a wide velocity variation across the transverse dimension of the electron beam so that the energy mismatch is considerable. The geometry to be studied is illustrated along with defined symbols in Fig. 1. The analysis will be applied to a consideration of near-synchronous waves and the effect of cyclotron waves will be neglected. In very thick beams the cyclotron waves can account for a considerable gain. The variational method used here can also be applied in a study of cyclotron wave excitation.

The usual assumptions are made in this small-signal analysis and in particular the potential along the rf structure is assumed to exhibit the following spatial and time dependence:

$$V(y,z,t)=V\Phi_0+\mathrm{Re}\sum_{n=1}^{N}\sqrt{2}V_n\Phi_n\exp(j\omega t-\Gamma_n z), \quad (2)$$

where V_n is independent of any space dimension and Φ_n is a function of y. Based on the above assumption, the electric field quantities exhibit the following dependence:

$$E_{zn}=\Phi_n\Gamma_n V_n, \quad (3)$$

$$E_{yn}=-V_n(\partial\Phi_n/\partial y). \quad (4)$$

The propagation constant $\Gamma_n=j\beta_e(1-jD_i\delta_n)$, where the δ_n are obtained from solutions of the dispersion equation for near-synchronous waves. The interaction

parameter is defined by

$$D_i^2=\frac{\omega}{\omega_c}\frac{KI_0G^2}{2V_0},$$

where

$$G^2=\frac{-\sinh j2\Gamma'(\bar{y}-y_s)}{2\sinh^2[j\Gamma'(y_d-y_s)]}.$$

The potential function in the regions between the sole and the lower beam edge and between the upper beam edge and the rf structure is found from the solutions to Laplace's equation and is conveniently written as

$$\Phi(y)=A\exp(j\Gamma_n y)+B\exp(-j\Gamma_n y), \quad \text{for } y_d\geq y\geq y_b. \tag{5}$$

Below the stream

$$\Phi_n=F\sinh jF_n(y-y_s), \quad \text{for } y_a\geq y\geq y_s. \tag{6}$$

The sole is considered to be a smooth, perfectly conducting surface and its potential is zero. Thus

$$\Phi_n(y=y_s)=0. \tag{7}$$

In general, the potential function within the stream may be conveniently expressed in terms of a power series solution as follows:

$$\Phi(y)=C\xi\left(1+\frac{\xi^2}{2}+\frac{5}{24}\xi^4+\cdots\right)+D\xi^2\left(1+\frac{\xi^2}{2}+\frac{11}{40}\xi^4+\cdots\right), \quad \text{for } y_b\geq y\geq y_a, \tag{8}$$

where $\xi_n\triangleq(\omega/\omega_c)+j\Gamma_n y$.

The constants A, B, C, D, and F in Eqs. (5) through (8) are yet to be determined from the transverse boundary conditions on $\Phi_n(y)$ at the sole, anode, and beam boundaries. Usually $|D|\ll|C|$ and hence the potential function within the stream is adequately represented by the truncated series

$$\Phi(y)\approx C\xi \quad \text{for } y_b\geq y\geq y_a. \tag{9}$$

The potential function is normalized to unity at the anode, $y=y_d$, assuming it to be an impedance sheet propagating a slow wave. For thicker streams additional terms in the power series must be retained. Thus from Eq. (5)

$$A=[\exp(j\Gamma_n y_d)+(B/A)\exp(-j\Gamma_n y_d)]^{-1}. \tag{10}$$

The constant in Eq. (8) is found to be

$$C=\{\xi_{an}[\cosh j\Gamma_n(y_d-y_b)]\}^{-1}\left(\frac{\xi_{bn}}{\xi_{an}}+H\frac{\xi_{an}}{\xi_{bn}}\right)^{-1} \tag{11}$$

where $H\triangleq\tanh j\Gamma_n(y_d-y_b)/\tanh j\Gamma_n(y_a-y_s)$, defining the beam position. It is convenient to define

$$T_n\triangleq[\cosh j\Gamma_n(y_d-y_b)][1+H(\xi_{an}/\xi_{bn})^2]^{-1}=\frac{\exp(j\Gamma_n y_b)+(B/A)\exp(-j\Gamma_n y_b)}{\exp(j\Gamma_n y_d)+(B/A)\exp(-j\Gamma_n y_d)} \tag{12}$$

and

$$S_n\triangleq(B/A)=\frac{\exp[-j\Gamma_n(y_d-y_b)]-T_n}{T_n-\exp[j\Gamma_n(y_d-y_b)]}\times\exp(2j\Gamma_n y_d). \tag{13}$$

The potential functions within the beam and in the region between the beam and the anode are now written as

$$\Phi_n(y)=(\xi_n/\xi_{bn})T_n, \quad \text{for } y_b\geq y\geq y_a \tag{14}$$

and

$$\Phi_n(y)=\frac{\exp(j\Gamma_n y)+S_n\exp(-j\Gamma_n y)}{\exp(j\Gamma_n y_d)+S_n\exp(-j\Gamma_n y_d)}, \quad \text{for } y_d\geq y\geq y_b. \tag{15}$$

The potential function is now matched at the lower beam boundary, $y=y_a$, using Eqs. (6) and (14):

$$F=\frac{\xi_{an}}{\xi_{bn}}\frac{T_n}{\sinh j\Gamma_n(y_a-y_s)}$$

and thus

$$\Phi_n(y)=T_n\frac{\xi_{an}}{\xi_{bn}}\frac{\sinh j\Gamma_n(y-y_s)}{\sinh j\Gamma_n(y_a-y_s)}, \quad \text{for } y_a\geq y\geq y_s. \tag{16}$$

The electric field components of interest in all three regions may now be obtained based on the assumed space-time dependence given in Eq. (2). The following definition is made:

$$E_n\triangleq\Gamma_n V_n=\Gamma_n V_n\Phi_n(y_d). \tag{17}$$

The field components are thus

$$E_{zn}(y)=E_n\frac{\exp j\Gamma_n y+S_n\exp(-j\Gamma_n y)}{\exp j\Gamma_n y_d+S_n\exp(-j\Gamma_n y_d)} \tag{18}$$

$$E_{yn}(y)=-jE_n\frac{\exp j\Gamma_n y-S_n\exp(-j\Gamma_n y)}{\exp j\Gamma_n y_d+S_n\exp(-j\Gamma_n y_d)} \tag{19}$$

for $y_d\geq y\geq y_b$,

$$E_{zn}(y)=E_nT_n\frac{\xi_n}{\xi_{bn}} \tag{20}$$

$$E_{yn}(y)=-jE_n\frac{T_n}{\xi_{bn}} \tag{21}$$

for $y_b\geq y\geq y_a$,

$$E_{zn}(y)=E_nT_n\frac{\xi_{an}}{\xi_{bn}}\frac{\sinh j\Gamma_n(y-y_s)}{\sinh j\Gamma_n(y_a-y_s)} \tag{22}$$

$$E_{yn}(y)=-jE_nT_n\frac{\xi_{an}}{\xi_{bn}}\frac{\cosh j\Gamma_n(y-y_s)}{\sinh j\Gamma_n(y_a-y_s)} \tag{23}$$

for $y_a\geq y\geq y_s$.

The component velocities u_{zn} and u_{yn} of the beam are obtained from a consideration of the Lorentz force equations in the beam, assuming linear perturbations on the average quantities. Since the y component of velocity depends upon the derivative of the potential function with respect to y, and the z component depends directly on the potential function, it is necessary to retain a second-order term in the potential function when dealing with u_{yn} and only a first-order term when obtaining u_{zn}. The velocity components are easily shown to be

$$u_{zn}=\frac{-\eta\Gamma_n V_n\Phi_n(y)}{j\omega_c\xi_n}=\frac{-\eta T_n E_n}{j\omega_c\xi_{bn}} \tag{24}$$

and

$$u_{yn}=\frac{\eta V_n}{j\omega_c\xi_n}\left[\frac{\partial\Phi_n(y)}{\partial y}+\frac{\omega_c\Gamma_n\Phi_n(y)}{j\omega_c\xi_n}\right]=\frac{\eta E_n T_n\xi_n}{\omega_c\xi_{bn}}. \tag{25}$$

The component electric fields present in the region between sole and anode in the absence of the beam are obtained as follows:

$$\Phi(y)=a\sinh j\Gamma'(y-y_s), \tag{26}$$

where Γ' is the cold-circuit propagation constant for the field component of interest. The potential function is again normalized to unity at the anode and hence

$$\Phi(y)=\frac{\sinh j\Gamma'(y-y_s)}{\sinh j\Gamma'(y_d-y_s)}. \tag{27}$$

The electric field components are obtained in a manner similar to that used when the beam is present. Define $E=\Gamma' V$. The y and z components of electric field are then

$$E_y(y)=-jE\frac{\cosh j\Gamma'(y-y_s)}{\sinh j\Gamma'(y_d-y_s)} \tag{28}$$

and

$$E_z(y)=E\frac{\sinh j\Gamma'(y-y_s)}{\sinh j\Gamma'(y_d-y_s)}. \tag{29}$$

The procedure to be applied in computing the excited wave amplitudes was outlined above and amounts to a minimization of the energy density associated with the mismatch in the presence of the beam. The average energy density associated with the mismatch is written using the field expressions as

$$W=\frac{\epsilon_0}{2(y_d-y_s)}\int_{y_s}^{y_d}\{|\sum_{n=1}^{3}E_{zn}-E_z|^2+|\sum_{n=1}^{3}E_{yn}-E_y|^2-\frac{\rho_0}{\epsilon_0\eta}[|u_{zn}|^2+|u_{yn}|^2]\}dy, \tag{30}$$

where the dc space-charge density ρ_0 is given by

$$\rho_0=-(\omega_c^2\epsilon_0/\eta).$$

In Eq. (30) E_y and E_z are the fields existing in the absence of the beam. In order to minimize the energy mismatch δW is formed and E_n and E_n^* are adjusted independently so that $\delta W=0$. The result of these variations of E_n and E_n^* is

$$\delta W=0=\frac{\epsilon_0}{2(y_d-y_s)}\int_{y_s}^{y_d}\delta\Big[(\sum_{n=1}^{3}E_{zn}-E_z)(\sum_{n=1}^{3}E_{zn}^*-E_z^*)+(\sum_{n=1}^{3}E_{yn}-E_y)(\sum_{n=1}^{3}E_{yn}^*-E_y^*)+\frac{\omega_c^2}{\eta^2}(u_{zn}u_{zn}^*+u_{yn}u_{yn}^*)\Big]dy. \tag{31}$$

The final result for calculating the excited wave amplitudes is expressed in matrix form as

$$\begin{Vmatrix}A_{11}&A_{21}&A_{31}\\A_{12}&A_{22}&A_{32}\\A_{13}&A_{23}&A_{33}\end{Vmatrix}\times\begin{Vmatrix}E_1\\E_2\\E_3\end{Vmatrix}=E_a\begin{Vmatrix}D_1^*\\D_2^*\\D_3^*\end{Vmatrix}, \tag{32}$$

where E_a = the total applied circuit field amplitude. The matrix elements are given by the following expressions:

$$A_{nm}=\frac{2\{\exp[j(\Gamma_n-\Gamma_m^*)y_d]-\exp[j(\Gamma_n-\Gamma_m^*)y_b]-S_nS_m^*\exp[-j(\Gamma_n-\Gamma_m^*)y_d]+S_nS_m^*\exp[-j(\Gamma_n-\Gamma_m^*)y_b]\}}{j(\Gamma_n-\Gamma_m)[\exp(j\Gamma_n y_d)+S_n\exp(-j\Gamma_n y_d)][\exp(-j\Gamma_m^* y_d)+S_n^*\exp(j\Gamma_m^* y_d)](y_d-y_s)}$$

$$+2\frac{T_nT_m^*}{\xi_{bn}\xi_{bm}^*}\left\{\left[\left(\frac{\omega}{\omega_c}\right)^2+1\right]\left(\frac{y_b-y_a}{y_d-y_s}\right)+\frac{j(\omega/\omega_c)(\Gamma_n-\Gamma_m^*)(y_b^2-y_a^2)}{2(y_d-y_s)}+\frac{\Gamma_n\Gamma_m^*}{3(y_d-y_s)}(y_b^3-y_a^3)\right\}$$

$$+\frac{2T_nT_m^*\xi_{an}\xi_{am}^*}{\xi_{bn}\xi_{bm}^*}\frac{\sinh j(\Gamma_n-\Gamma_m^*)(y_a-y_s)}{j(\Gamma_n-\Gamma_m^*)(y_d-y_s)[\cosh j(y_a-y_s)(\Gamma_n-\Gamma_m^*)-\cosh j(y_a-y_s)(\Gamma_n+\Gamma_m^*)]}, \tag{33}$$

and

$$D_n=\frac{\exp[j(\Gamma_n-\Gamma'^*)y_a+j\Gamma'^*y_s]-\exp[j(\Gamma_n-\Gamma'^*)y_b+j\Gamma'^*y_s]+S_n\exp-[j(\Gamma_n-\Gamma'^*)y_d+j\Gamma'^*y_s]-S_n\exp-[j(\Gamma_n-\Gamma'^*)y_b+j\Gamma'^*y_s]}{j(\Gamma_n-\Gamma'^*)[\sinh-j\Gamma'^*(y_d-y_s)][\exp(j\Gamma_n y_d)+S_n\exp(-j\Gamma_n y_d)](y_d-y_s)}$$

$$+\frac{T_n}{\xi_{bn}\sinh-j\Gamma'^*(y_d-y_s)}\left\{\frac{\omega}{\omega_c}\frac{[\cosh-j\Gamma'^*(y_b-y_s)-\cosh-j\Gamma'^*(y_a-y_s)]}{-j\Gamma'^*(y_d-y_s)}\right.$$

$$+\frac{j\Gamma_n[y_b\cosh-j\Gamma'^*(y_b-y_s)-y_a\cosh-j\Gamma'^*(y_a-y_s)]}{-j\Gamma'^*(y_d-y_s)}+\frac{j\Gamma_n[\sinh-j\Gamma'^*(y_b-y_s)-\sinh-j\Gamma'^*(y_a-y_s)]}{\Gamma'^{*2}(y_d-y_s)}$$

$$\left.+\frac{\sinh-j\Gamma'^*(y_b-y_s)-\sinh-j\Gamma'^*(y_a-y_s)}{-j\Gamma'^{*2}(y_d-y_s)}\right\}$$

$$+\frac{2T_n\xi_{an}\sinh j(\Gamma_n-\Gamma'^*)(y_a-y_s)}{\xi_{bn}j(\Gamma_n-\Gamma'^*)(y_d-y_s)\{\cosh j[(y_a-y_s)\Gamma_n-\Gamma'^*(y_d-y_s)]-\cosh j[(y_a-y_s)\Gamma_n+\Gamma'^*(y_d-y_s)]\}}. \quad (34)$$

In order to facilitate the calculation of parameters for the dispersion equation and the matrix elements, the following definitions of variables are made. Quantities are normalized with respect to the interaction width, (y_d-y_s), as the space-charge flow may originate from a cathode located below the plane of the sole, i.e., $y<y_s$.

$$\alpha\triangleq y_a/(y_d-y_s), \quad (35)$$

$$\beta\triangleq y_b/(y_d-y_s), \quad (36)$$

$$\psi\triangleq y_d/(y_d-y_s). \quad (37)$$

The wave propagation constant $j\Gamma_n$ and the interaction parameters may now be written in terms of α, β, and ψ as

$$j\Gamma_n=-\left(\frac{\omega}{\omega_c}\right)\left(\frac{2}{\alpha+\beta}\right)\frac{(1-jD_i\delta_n)}{(y_d-y_s)}, \quad (38)$$

$$D_i^2=\frac{\beta-\alpha}{\beta+\alpha}\frac{\sinh\left[\frac{2\omega}{\omega_c}\frac{(2+\alpha+\beta-2\psi)}{(\alpha+\beta)}\right]}{\sinh[(4\omega/\omega_c)(\alpha+\beta)^{-1}]}, \quad (39)$$

$$r=D_i^{-1}[(\beta-\alpha)/(\beta+\alpha)], \quad (40)$$

and

$$H=\tanh\left[\frac{2\omega}{\omega_c}\frac{(\psi-\beta)}{(\alpha+\beta)}\right]\Big/\tanh\left[\frac{2\omega}{\omega_c}\frac{(1-\psi+\alpha)}{(\alpha+\beta)}\right]. \quad (41)$$

The following terms ξ_{an}, ξ_{bn}, T_n, and S_n are involved in the calculation of the matrix elements:

$$\xi_{an}=\frac{\omega}{\omega_c}-\frac{\omega}{\omega_c}(1-jD_i\delta_n)\frac{2\alpha}{\alpha+\beta}, \quad (42)$$

$$\xi_{bn}=\frac{\omega}{\omega_c}-\frac{\omega}{\omega_c}(1-jD_i\delta_n)\frac{2\beta}{\alpha+\beta}, \quad (43)$$

$$T_n=\left\{\cosh\left[\frac{2\omega}{\omega_c}(1-jD_i\delta_n)\frac{\psi-\beta}{\alpha+\beta}\right]\left[1+H\left(\frac{\xi_{an}}{\xi_{bn}}\right)^2\right]\right\}^{-1}, \quad (44)$$

and

$$S_n=\left\{\frac{\exp\left[\frac{2\omega}{\omega_c}(1-jD_i\delta_n)\frac{\psi-\beta}{\alpha+\beta}\right]-T_n}{T_n-\exp\left[\frac{-2\omega}{\omega_c}(1-jD_i\delta_n)\frac{\psi-\beta}{\alpha+\beta}\right]}\right\}\times\exp\left[\frac{-4\omega}{\omega_c}(1-jD_i\delta_n)\frac{\psi}{\alpha+\beta}\right]. \quad (45)$$

Equations (42)–(45) are for $n=1, 2, 3$. The matrix elements are now calculated for $n=1, 2, 3$; $m=1, 2, 3$ where $A_{nm}=A_{mn}^*$.

A solution of the matrix expression, Eq. (32), gives the electric field amplitudes of the excited waves which are related to the wave voltage amplitudes as follows:

$$\frac{V_n}{V_a}=\frac{[1+D_i(b+jd)]}{[1-jD_i\delta_n]}\frac{E_n}{E_a}, \quad (46)$$

where b = injection velocity parameter, and d = circuit wave loss parameter.

Once the excited wave amplitudes for a minimum-energy mismatch for a given beam configuration and amount of space charge have been calculated, the effect on the starting current of a magnetron backward-wave oscillator may be found by determining the point along the anode rf structure at which the total rf wave amplitude becomes zero. The propagation of electromagnetic waves along the anode is given by

$$\frac{V_t(\theta)}{V_a}=\exp\left(-j\frac{\theta}{D_i}\right)\sum_{n=1}^{3}\frac{V_n}{V_a}\exp(-\theta\delta_n), \quad (47)$$

TABLE I. Energy mismatch and M-BWO starting conditions for finite-thickness streams ($d=0$).

			Approximate match			Variational procedure		
H	r	ω/ω_c	b	D_iN	$W/(\epsilon_0E^2/2)$	b	D_iN	$W/(\epsilon_0E^2/2)$
1	0.1	2	0	0.249	0.199×10^{-4}	0.0099	0.250	0.199×10^{-4}
1	0.3	2	0	0.247	0.179×10^{-3}	0.0232	0.250	0.178×10^{-4}
1	0.5	2	0	0.242	0.494×10^{-3}	0.0148	0.249	0.493×10^{-3}
1	1.0	2	0	0.225	0.458×10^{-1}	−0.2540	0.245	0.212×10^{-2}
1	0.1	1	0	0.249	0.104×10^{-2}	0.0796	0.250	0.103×10^{-2}
1	0.3	1	0	0.247	0.936×10^{-2}	0.1964	0.255	0.880×10^{-2}
1	0.5	1	0	0.242	0.260×10^{-1}	0.1786	0.265	0.240×10^{-1}
1	0.1	0.5	0	0.249	0.853×10^{-2}	0.1807	0.249	0.821×10^{-2}
1	0.3	0.5	0	0.247	0.769×10^{-1}	0.4423	0.252	0.594×10^{-1}
1	0.5	0.5	0	0.242	0.210	0.3244	0.271	0.155
0.5	0.1	2	−0.067	0.249	0.103×10^{-1}	0.7056	0.239	0.927×10^{-2}
0.5	0.5	2	−0.323	0.242	0.765×10^{-1}	0.8825	0.259	0.435×10^{-1}
0.5	1	2	−0.607	0.226	0.115	−1.079	0.303	0.163
0.5	0.1	1	−0.067	0.249	0.167×10^{-1}	0.4150	0.246	0.154×10^{-1}
0.5	0.5	1	−0.323	0.242	0.203	0.7110	0.265	0.978×10^{-1}
0.5	0.1	0.5	−0.067	0.249	0.423×10^{-1}	0.3390	0.246	0.375×10^{-1}
0.5	0.5	0.5	−0.323	0.242	0.853	0.5190	0.266	0.272
2	3	1	1.513	0.165	0.492×10^{-3}	7.21	0.162	0.291×10^{-3}
2	4	1	1.921	0.145	0.280×10^{-2}	8.52	0.134	0.166×10^{-3}
2	5	1	2.32	0.129	0.192×10^{-2}	9.65	0.114	0.116×10^{-3}

where $\theta\triangleq 2\pi D_iN_s$. An oscillation will exist, i.e., the right-hand side of Eq. (47) will be zero, for some combination of b and θ for a given set of H, r, and d.

THIN-STREAM WAVE AMPLITUDES AND OSCILLATION CONDITIONS

If the stream is extremely thin as compared to the interaction width between the sole and anode, it is permissible to treat the input boundary value problem in an approximate manner and match at only one or two levels of the stream. Matching the two velocity components at the beam edge and the field components at the anode gives rise to the following matrix for the excited wave amplitudes:

$$\begin{Vmatrix} 1 & 1 & 1 \\ S_n-1 & S_{n+1}-1 & S_{n+2}-1 \\ \dfrac{jS_n}{\delta_n} & \dfrac{jS_{n+1}}{\delta_{n+1}} & \dfrac{jS_{n+2}}{\delta_{n+2}} \end{Vmatrix} \begin{Vmatrix} V_n \\ V_{n+1} \\ V_{n+2} \end{Vmatrix} = \begin{Vmatrix} V_a \\ 0 \\ 0 \end{Vmatrix}, \quad (48)$$

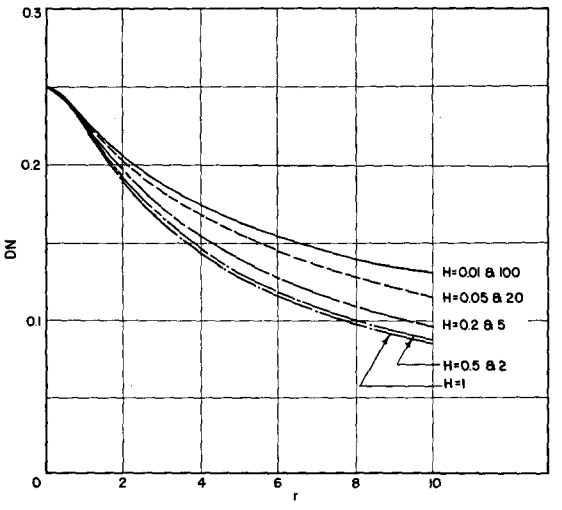

FIG. 2. Thin stream starting conditions ($d=0$).

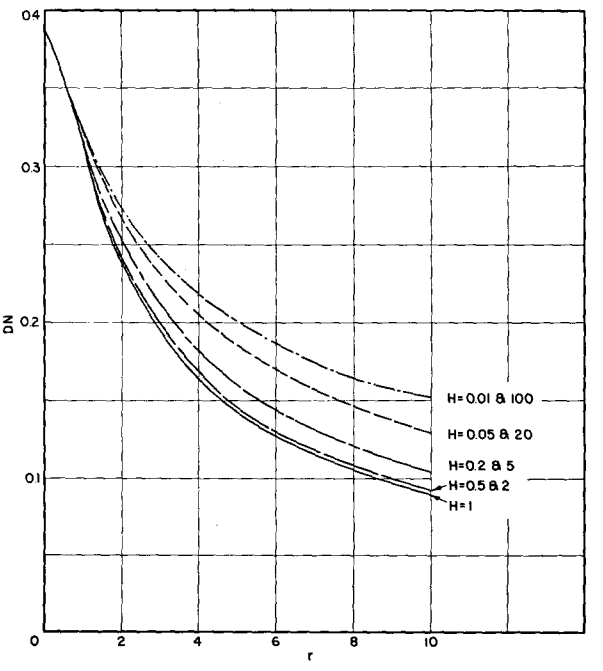

FIG. 3. Thin stream starting conditions ($d=1.0$).

TABLE II. Energy mismatch and M-BWO starting conditions for finite thickness streams with circuit loss.

				Approximate match			Variational procedure		
H	r	ω/ω_c	d	b	D_iN	$W/(\epsilon_0E^2/2)$	b	D_iN	$W/(\epsilon_0E^2/2)$
1	0.1	2	0.1	0	0.258	0.199×10^{-4}	0.0091	0.258	0.199×10^{-4}
1	0.5	2	0.1	0	0.250	0.494×10^{-3}	0.0133	0.257	0.493×10^{-3}
1	1	2	0.1	0	0.231	0.198×10^{-2}	−0.2434	0.251	0.212×10^{-2}
1	0.1	1	0.1	0	0.258	0.104×10^{-2}	0.0735	0.259	0.103×10^{-2}
1	0.5	1	0.1	0	0.250	0.260×10^{-1}	0.1643	0.273	0.240×10^{-1}
1	1	1	0.1	0	0.231	0.122	−0.940	0.285	0.354
1	0.1	0.5	0.1	0	0.258	0.853×10^{-2}	0.1668	0.258	0.823×10^{-2}
1	0.5	0.5	0.1	0	0.250	0.210	0.306	0.280	0.158
1	0.1	2	0.5	0	0.299	0.199×10^{-4}	0.0063	0.299	0.199×10^{-4}
1	0.5	2	0.5	0	0.286	0.494×10^{-3}	0.0081	0.294	0.494×10^{-3}
1	1	2	0.5	0	0.260	0.198×10^{-2}	−0.1973	0.281	0.209×10^{-2}
1	0.1	1	0.5	0	0.299	0.104×10^{-2}	0.051	0.300	0.103×10^{-2}
1	0.5	1	0.5	0	0.286	0.256×10^{-1}	0.115	0.313	0.245×10^{-1}
1	0.1	0.5	0.5	0	0.299	0.851×10^{-2}	0.116	0.300	0.831×10^{-2}
1	0.5	0.5	0.5	0	0.286	0.199	0.233	0.324	0.162
0.5	0.1	2	0.1	−0.067	0.258	0.103×10^{-1}	0.615	0.246	0.934×10^{-2}
0.5	0.5	2	0.1	−0.323	0.250	0.764×10^{-1}	0.774	0.272	0.455×10^{-1}
0.5	0.1	1	0.1	−0.067	0.258	0.167×10^{-1}	0.369	0.253	0.155×10^{-1}
0.5	0.5	1	0.1	−0.323	0.250	0.202	0.633	0.275	0.102
0.5	0.1	2	0.5	−0.067	0.299	0.103×10^{-1}	0.365	0.281	0.971×10^{-2}
0.5	0.5	2	0.5	−0.321	0.287	0.764×10^{-1}	0.397	0.324	0.538×10^{-1}
0.5	0.1	1	0.5	−0.067	0.299	0.167×10^{-1}	0.222	0.288	0.159×10^{-1}
0.5	0.5	1	0.5	−0.321	0.287	0.192	0.376	0.317	0.118
0.5	0.1	0.5	0.5	−0.067	0.299	0.419×10^{-1}	0.185	0.293	0.388×10^{-1}
0.5	0.5	0.5	0.5	−0.321	0.287	0.656	0.272	0.320	0.324

where

$$\delta_{n+3}=\delta_n$$

and

$$S_n=-(r-j\delta_n)(b+j\delta_n).$$

A solution of the above matrix for the wave amplitudes yields

$$V_n/V_a=X_n/\sum_{n=1}^{3}X_n, \tag{49}$$

where

$$X_n=\frac{j(S_{n+1}-1)S_{n+2}}{\delta_{n+2}}-\frac{j(S_{n+2}-1)S_{n+1}}{\delta_{n+1}}.$$

The rf voltage as a function of distance is again given by Eq. (47), where the excited wave amplitudes are calculated by Eq. (49). The starting conditions for the thin-stream M-BWO have been calculated as a function of space charge, beam location, and circuit loss. These results are presented in Figs. 2 through 6. Circuit loss increases the required starting length for low space-charge conditions and has little effect with large space-charge fields. For finite values of d the starting length is constant for streams located at H and $1/H$. The $(\beta-\beta_e)L$ curves are symmetric with respect to H and relatively independent of circuit loss.

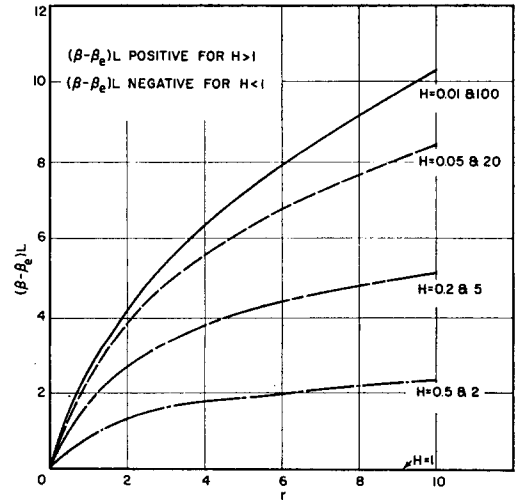

FIG. 4. $(\beta-\beta_e)L$ vs r at start oscillation $(d=0)$.

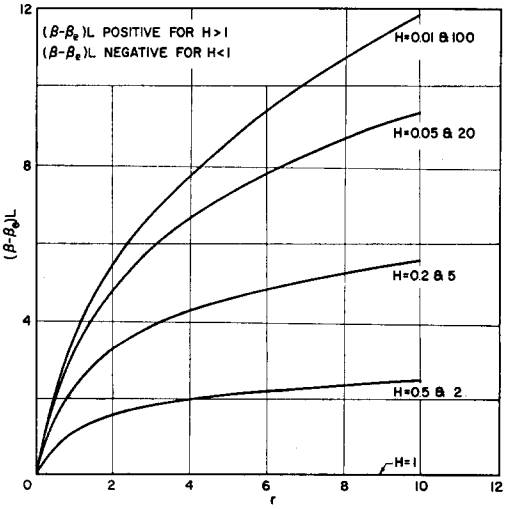

FIG. 5. $(\beta-\beta_e)L$ vs r at start oscillation $(d=1.0)$.

EFFECT OF ENERGY MISMATCH ON STARTING (THICK BEAMS)

The average energy density associated with the mismatch occurring when the electron stream is introduced between the sole and anode was given by the integral of Eq. (30). The integral is easily evaluated and the average energy density in the mismatch is given by

$$W=\frac{\epsilon_0 E^2}{2}\left\{\sum_{n,m=1}^{3} A_{nm}\left(\frac{E_n}{E}\right)\left(\frac{E_n}{E}\right)^{*}-\sum_{n=1}^{3} D_n\left(\frac{E_n}{E}\right)-\sum_{n=1}^{3} D_n^{*}\left(\frac{E_n}{E}\right)^{*}\right.$$

$$\left.+\frac{\sinh\dfrac{(4\omega/\omega_c)(1+D_i b)}{\alpha+\beta}}{2\dfrac{\omega}{\omega_c}\dfrac{(1+D_i b)}{\alpha+\beta}\left[\cosh\dfrac{4\omega}{\omega_c}\dfrac{(1+D_i b)}{\alpha+\beta}-\cos\dfrac{4\omega}{\omega_c}\dfrac{D_i(y_a-y_s)}{\alpha+\beta}\right]}\right\}, \quad (50)$$

where the electric field of the first term is that present at the anode of the unperturbed circuit at $z=0$. The factor $\epsilon_0 E^2/2$ is approximately unity. The integrated energy density (average) appears in the cutoff waves which arise in the presence of the electron stream. These fields provide for a perfect match at the input boundary when coupled with the fields associated with the near-synchronous waves excited. Of course, the energy density associated with the cutoff modes is highest at the electron stream itself. Hershenov[5,6] has determined the variation of energy mismatch across the stream, for the M-FWA (forward-wave amplifiers), and has calculated the change in excited wave amplitudes.

The minimum-energy method has been used to calculate the excited wave amplitudes and starting conditions for the M-BWO. This method is particularly useful when the transverse velocity variation across the stream is large. The results are compared with the approximate match results for no circuit loss in Table I. The energy mismatch for both calculations is given. The average energy density mismatch W is normalized with respect to $\epsilon_0 E^2/2$, which is approximately unity. The effects in the presence of rf circuit loss are shown in Table II. The magnitude and degree of influence of the energy mismatch on M-BWO starting conditions is apparent from Tables I and II.

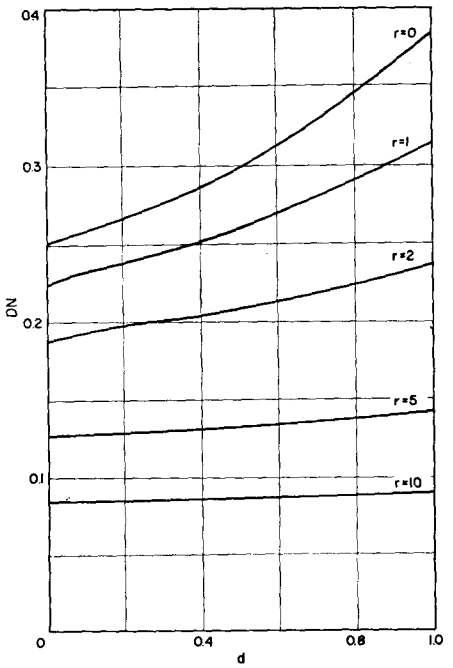

FIG. 6. Effect of loss on starting length ($H=1$).

It is clear that the required starting length is greater when calculated by the variational procedure and that the amplitudes of the cutoff waves excited increase with increasing space-charge field strength relative to the circuit fields. Generally the required injection velocity is also higher, except that under some large space-charge field conditions the required b value is less, sometimes even falling below synchronism.

This variational treatment of the input boundary value problem predicts that the starting length for an M-BWO increases as the beam thickness is increased, which is contrary to the predictions of the previous linear theories. This increase in required length is attributable to a lack of phase focusing in thick-beam devices and, hence, a less favorable interaction. This reduced interaction results in a decrease in the beam loading on the rf structure and, hence, the required beam velocity would be higher. Similar effects in thick-beam forward-wave amplifiers have been found by Gandhi.[8]

It is interesting to note that for signal frequencies above the cyclotron frequency the percentage mismatch is small, whereas for $\omega/\omega_c<1$ the effect is accentuated, and under some conditions the average energy density

[8] O. P. Gandhi, "Multiple stream crossed-field interaction" [to be published in J. Electronics and Control (London)].

mismatch amounts to over 20% of the electrostatic field energy in the absence of the beam. It may also be that under these conditions the cyclotron waves are excited to an appreciable extent. These have not been accounted for in this analysis.

The effect of rf circuit attenuation is to accentuate nearly all of the above trends as indicated in Table II.

CONCLUSIONS

The energy mismatch occurring and the cutoff waves excited due to the introduction of an M-type space charge flow in the anode-sole region of a planar crossed-field oscillator were calculated using Thomson's theorem in the solution of the input boundary value problem. This variational technique is shown to be particularly useful when the transverse velocity variation in the beam is large.

The cutoff wave amplitudes excited are increased as the velocity spread is increased and as the circuit attenuation is increased. The required starting length is greater for thick-beam tubes. The effect of the mismatch is greatest for signal frequencies less than the cyclotron frequency. This variational technique may conveniently be applied to any two-dimensional space-charge flow.

ACKNOWLEDGMENTS

The authors are extremely grateful to L. Flanigan and A. Pajas for their work in programming the problem for the IBM-704 computer.

JOURNAL OF APPLIED PHYSICS VOLUME 33, NUMBER 1 JANUARY, 1962

Investigation of the Coercive Forces of Ni, Fe, and Ni-Fe Films during Evaporation

KLAUS H. BEHRNDT*
IBM Federal Systems Division, Kingston, New York
(Received July 3, 1961)

The dependence of the coercive force of Ni, Fe, and Ni-Fe films upon film thickness and amount of trapped gas was evaluated *in vacuo*. The magneto-optic Kerr effect was utilized for this investigation. Although the penetration depth of light into the film material was determined to be 150±25 A, measurements of H_c could commence for film thicknesses <100 A. It was found that the coercive force H_c is independent of film thickness if the content of trapped gas, as indicated by the p/r (residual gas pressure over deposition rate) ratio is very small, e.g., 5×10^{-8} torr/A/sec for Ni films. At higher p/r ratios, the coercive force of Ni films displays initially a steep rise which is followed by a shallow minimum, while in Ni-Fe films a maximum appears at about 750 A. The different behavior of Fe films is ascribed to higher gas absorption on this material rather than a principal change in the mechanism of the coercive force. A hypothesis is proposed as explanation for the observed effects.

I. INTRODUCTION

FOR a number of years it was expected that the magnetic properties of thin films were influenced by the amount of gas trapped during film fabrication. Furthermore, if the properties are not measured *in vacuo* and immediately after deposition, oxidation and penetration of gas into the interior of the film may change the results appreciably.

To investigate the questions implied in these statements, the apparatus employed must allow to: (a) maintain ultra-high vacua during the evaporation, and (b) measure the magnetic film properties during and after the deposition *in vacuo* with a sensitivity sufficient to yield data for films which are only a few atomic layers thick.

II. APPARATUS

An evaporation system was constructed out of glass.[1] Two tubes of $2\frac{3}{4}$-in. diameter were fused into a cross. The horizontal tube contained the shutter, connection to ionization gauge, and cyro pump, while evaporation source and substrate were located in the vertical tube, which is shown in cross section in Fig. 1. The evaporation source consisted of two concentric rings of the evaporant wire, and depositions were performed by subliming from the resistance heated wire. In each "run" four films of 1-cm diameter were deposited, together with a "monitor strip" for measuring resistance

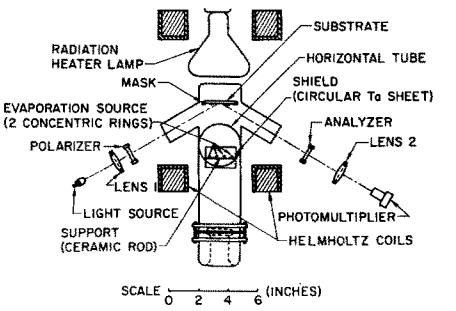

FIG. 1. Cross section (schematic) through vacuum chamber and Kerr-effect apparatus.

* Present address: General Dynamical Astronautics, San Diego, California.

[1] For a detailed description of the evaporation system see K. H. Behrndt, Vacuum Symposium Transactions (1959), p. 255.